American Journal of Science

SEPTEMBER 2008

FEEDBACKS AMONG CLIMATE, EROSION, AND TECTONICS IN A CRITICAL WEDGE OROGEN

GERARD H. ROE*, KELIN X. WHIPPLE**, and JENNIFER K. FLETCHER***

ABSTRACT. The interactions among climate, erosion, and tectonics have long been of interest to geologists, but have not yet been united into a single theoretical framework. In this study, representations of orographic precipitation and fluvial erosion are combined with the concept of a critical wedge orogen. The idealized framework captures the basic system dynamics. It also allows for a formal analysis of the precipitation and tectonic interactions in terms of feedback factors and gains, and so permits a quantitative comparison of their relative strengths. The constraint of self-similar growth in a critical wedge orogen acts as a tectonic governor, whereby changes in orogen size are strongly damped. We determine that this negative tectonic feedback is stronger than the precipitation feedback, which may be negative or positive depending on whether precipitation increases or decreases with orogen size. For an extreme positive feedback unconstrained runaway growth is possible, ultimately leading to plateau formation. When orographic precipitation leads to a significant rain shadow, there is a strong partitioning of rock uplift rates that favors the wet, windward flank of the orogen. This flank also dominates the response of the whole orogen to changes in climate or tectonic forcing, except in the case where a large fraction of the eroded material is recycled into the wedge. Finally, it is demonstrated that the response time of the orogen depends on the feedbacks, and is proportional to the gain of the system.

1. INTRODUCTION

An active mountain range reflects the competition of opposing tendencies. Tectonic convergence adds mass to the system, and erosional fluxes remove it. The erosion depends on a climate that is itself controlled by the topography. For these reasons, the proposition that interactions must exist among climate, erosion, and tectonics has been much discussed. It is a dramatic idea and speculations about the nature of the interactions go back to the beginning of the geological literature. It has become an increasingly active area of research in recent years (fig. 1).

Many observational studies have presented correlations among exhumation, topography, and climate (Adams, 1980; Suppe, 1980; Koons, 1990; Masek and others, 1994; Brandon and others, 1998; Montgomery and others, 2001; Reiners and others, 2003). Such associations are suggestive, but without a physical model, the separate possibilities of cause, effect, and coincidence cannot be distinguished. A few numerical models have been employed to explore the feedbacks (Koons, 1989; Beaumont and others, 1992; Masek and others, 1994; Willett, 1999a; Stolar and others, 2006). What has been missing is a theoretical framework through which the observations can be interpreted, and which can reveal the functional dependencies of the numerical modeling efforts and evaluate their general applicability.

*Department of Earth and Space Sciences, University of Washington, Seattle, Washington 98195; gerard@ess.washington.edu
**School of Earth and Space Exploration, Arizona State University, Tempe, Arizona 85287
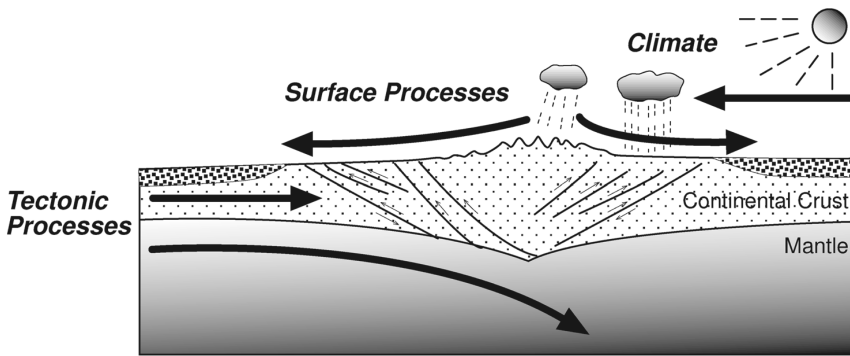***Department of Atmospheric Sciences, University of Washington, Seattle, Washington 98195

Fig. 1. Overview of the processes involved in the dynamics of an active orogen (after Willett, 1999; and Roe and others, 2006).

Recently, several analytical studies (Hilley and others, 2004; Whipple and Meade, 2004; Roe and others, 2006) have addressed the interactions between the tectonic and erosion components of the system. Although climate forcing of the system was prescribed and fixed, these studies demonstrated that tectonic-erosion interactions alone give rise to strong constraints on the system dynamics, and that the constraints are likely to operate under a wide range of conditions. The present study quantifies these tectonic-erosion interactions in terms of a formal feedback analysis, and extends the framework to incorporate a precipitation rate that varies as a function of orogen size. The framework makes predictions, for example; of how rock uplift patterns vary with the strength of a rain shadow that is, itself, a function of the orogen size. The value of a feedback analysis is that it allows for a quantification and comparison of the relative strengths of the tectonic and climate interactions.

The analytical studies of Hilley and others (2004), Whipple and Meade (2004), and Roe and others (2006) take advantage of the concept of a Coulomb critical wedge orogen (for example, Chapple, 1978; Davis and others, 1983; Dahlen, 1984, 1990). Under the assumption that the crust behaves as a Coulomb plastic material there is instantaneous deformation wherever gravitational stresses exceed the yield stress. Assuming a time-invariant geometry for the basal decollement, the result is an orogen that maintains a self-similar critical topographic form as it grows or shrinks. Furthermore, if the decollement is planar this critical topographic form is wedge-shaped, and the mean cross-sectional profile maintains a constant taper angle. Many orogenic belts have forms approximating that predicted by Coulomb critical wedge theory (for example, Dahlen, 1990; Willett, 1999a; Whipple and Meade, 2004). Laboratory sand-box experiments and numerical models also support the theory's relevance for the dynamic evolution of mountain ranges (for example, Koons, 1990; Willet and others, 1993; Willett, 1999a; Stolar and others, 2006). The particular power of the critical wedge framework is that it provides an essentially geometrical description of tectonics. In combination with simple models of erosion (also a function of orogen geometry), this allows for an evaluation of the relative roles of climatic and tectonic factors controlling the orogen size, strain rate patterns, particle trajectories, and rock uplift rates.

The most straightforward situation to consider is one where fluvial erosion is commonly represented by an expression of the form $\dot{e} = KQ^mS^n$, where $\dot{e}$ is the erosion rate, Q is geomorphically-effective discharge, S is the downstream slope, K is rock erodibility, and m and n are constants reflecting the physics of the dominant erosion process (for example, Whipple and Tucker, 1999). Discharge, in turn, can be repre-

sented as $Q = P \cdot kx^h$, where P is the average precipitation rate, x is the along-channel distance from the divide, and kx^h is the contributing upstream drainage area (Hack, 1957). We have made the simplifying assumption that the geomorphologically-effective discharge scales linearly with mean annual precipitation. While we note that the relation between erosion and mean annual precipitation is not quantitatively known, this assumption is reasonable and such a relation is necessary to link orographic precipitation, erosion, and orogen evolution. We do explore the consequences of a range in the discharge exponent, m. In effect, this exponent encapsulates both the relation between mean annual precipitation and the geomorphologically-effective discharge and the relation between this discharge and erosion rate. This erosion rule is one of many that have been proposed, and has some well known limitations (see for example, Whipple 2004), but it is adequate for the approach taken in this paper. The case of glacial erosion is left to the Discussion.

In equilibrium, a mass balance must exist between the accretionary flux into the orogen and the erosional flux (or yield) from the orogen. Requiring this balance yields a scaling relationship for the width of the orogen, L, in terms of the accretionary flux, F, and the precipitation rate, P. Although the models of Hilley and others (2004), Whipple and Meade (2004), and Roe and others (2006) differ in some respects, they all produce essentially the same result:

$$F = \eta L^{1+hm} P^m, \qquad (1)$$

where η is a constant that depends on rock erodibility, orogen geometry, and several other model parameters. Further analysis shows that the formula is insensitive to the model details (Whipple and Meade, 2004; Roe and others, 2006), and in particular does not depend on the distribution of rock uplift rates across the orogen, provided it also varies self-similarly.

A result to emphasize from these studies is that the requirement of self-similar form acts as a 'tectonic governor' (for example, Maxwell, 1868), strongly damping the system response to changes in forcing. Given an increase in erosion, for example, the orogen will shrink in both height and width. All else being equal, the same accretionary flux is now distributed over a smaller width, and so the local rock uplift rates must increase. This acts to oppose the effects of the increase in erosion, and hence is a negative feedback on the orogen size. This basic physical mechanism is a strong constraint on the system dynamics, and its operation essentially depends only on there being some tendency for the orogen to grow self-similarly (that is, as an orogen builds up it also builds out), and some tendency for erosion to increase with increasing discharge and channel slope. The concepts have been applied to a fold-and-thrust belt in the Andes (Hilley and others, 2004), to Taiwan (Whipple and Meade, 2006), and to the Olympic Mountains of Washington State (Stolar and others, 2007a), and a glacial-erosion version to the southern Alps of New Zealand (Tomkin and Roe, 2007). Coupled numerical models of crustal deformation and landscape evolution also obey the scaling relationship very closely (Stolar and others, 2006), suggesting that, although severe assumptions were used in its derivation, the scaling relationship captures the important behavior, despite the many possible degrees of freedom by which the numerical system might adjust (and by analogy, the richer natural system).

The value of the simple approach used here is that it provides a straightforward and self-consistent framework for exploring the potential magnitude of the interactions, one in which the dependencies can be clearly understood. As such it is not intended as a simulation of any particular orogen or setting, but rather as a tool to provide greater fundamental understanding and for the interpretation of complex numerical simulations of the fully-coupled system. The implications and limitations of the model are addressed in the last section of this paper.

2. FEEDBACK BASICS

Standard feedback analysis is an effective method for characterizing the strengths of interactions in coupled systems (for example, Hansen and others, 1984; Schlesinger, 1985; Torne and Harte, 2006; Roe and Baker, 2007), and borrows terminology and definitions from op-amp theory in electronics (for example, Bode, 1945; Delaney, 1969; Brophy, 1983)[1]. In general terms, a feedback is a physical process, which when added to a reference physical system acts to make the input a function of the output. In a feedback analysis, it is critical that definitions are clearly stated and consistently applied, both in terms of what the reference physical system is, and also what the input and output variables of interest are. This is not a flaw in the analysis method: keeping close track of how the system is dissected to study the individual interactions is essential in dynamical systems where everything influences everything else. Roe (Feedbacks, timescales, and seeing red, unpublished manuscript) gives a general review of the analysis method, and so here we give only a brief introduction and specifically as it relates to orogen dynamics.

We begin by defining a general sensitivity parameter, λ_L, as the change in the width of the orogen per unit change in the accretionary flux:

$$\Delta L = \lambda_L \Delta F, \tag{2}$$

where the subscript L has been used to make it clear the sensitivity factor refers to width changes. Defining orogen sensitivity and feedbacks in terms of orogen size is simply a choice we have made, and in a subsequent section a sensitivity factor for rock uplift is defined. As is emphasized in Section 5 and Roe (Feedbacks, timescales, and seeing red, unpublished manuscript), if different choices are made, the magnitude and even the size of the feedbacks can change. (1) governs the steady-state relationship between F, L, and P. We are interested in how perturbations of the system (that is, climate or tectonic forcing) are balanced by changes in other parts of the system. To that end, a first order Taylor series expansion of this scaling relationship can be written as:

$$\Delta F = \frac{\partial F}{\partial L} \Delta L + \frac{\partial F}{\partial P} \Delta P \tag{3}$$

where ΔF, ΔP, ΔL represent some small change in the flux, the width, and the precipitation, respectively. (3) can be thought of as a perturbation balance equation: for an imposed change in any one variable, it shows the combination of changes that must come about in the other two variables for the new equilibrium to be established.

First, consider the case where there is no precipitation feedback. The imposed precipitation rate is constant and does not vary with the shape of the wedge (that is, $\Delta P = 0$). In which case the no-feedback sensitivity parameter, λ_L^0, can be obtained by combining (2) and (3) to give:

$$\lambda_L^0 = \frac{1}{\left(\dfrac{\partial F}{\partial L}\right)}. \tag{4}$$

Using (1), and taking advantage of the simple expressions for the derivatives of power-law relationships, the above can be written as

---

[1] Definitions of feedback factors and gains can sometimes be frustratingly different (for example, Hansen and others, 1984). Here we use the standard definitions from electronics.

$$\lambda_L^0 = \frac{1}{(1 + hm)} \frac{L}{F}.$$ (5)

To recap, λ_L^0 reflects the sensitivity of the wedge width to a change in the accretionary flux, in the case that precipitation remains unchanged. An important result to note is that this sensitivity is not constant but varies as a function of the width and the flux. In power law relationships of the form of (1), it is fractional changes in the variables that balance each other, not the absolute changes. Setting $\Delta P = 0$, and combining (5) and (3) gives

$$\frac{\Delta L}{L} = \frac{1}{1 + hm} \frac{\Delta F}{F}.$$ (6)

So, for example, (5) and (6) show that the larger the wedge is, the more sensitive it is to a change in tectonic forcing (that is, ΔF). In other words, the bigger the orogen the greater must be the change in its width (that is, ΔL) to accommodate a given change in flux. A physical interpretation of this is that, for a given F, a larger L implies a lower P [because of (1)]. The system therefore has less ability to erode away an increase in F, and a greater change in L results.

Conversely the greater the magnitude of the flux, the smaller the change in width required to accommodate it: for a given L, a larger F implies a larger P. Consequently the system has a greater ability to erode away changes in forcing, and so it is less sensitive.

The product of the exponents hm in (5) reflects the dependency of fluvial erosion on discharge and drainage basin geometry. The larger hm is, the more effectively erosion is able to accommodate the change in flux, and so the smaller the resulting change in width. Note that λ_L^0 is always positive.

2.1. A Precipitation Feedback

The effect of a precipitation feedback can be analyzed by supposing that P is not constant but instead varies as a function of orogen width [that is, $P = P(L)$], and asking how the value of λ_L changes.

For sufficiently small changes $\Delta P = dP/dL \cdot \Delta L$, and so (3) becomes

$$\Delta F = \Delta L \left(\frac{\partial F}{\partial L} + \frac{\partial F}{\partial P} \frac{dP}{dL} \right).$$ (7)

Using (7), (1), and (2) then, the sensitivity parameter in the case of a feedback is

$$\lambda_L = \frac{\lambda_L^0}{1 + \dfrac{m\lambda_L^0 F}{P} \left(\dfrac{dP}{dL} \right)},$$ (8)

which using (5) can be written as

$$\lambda_L = \frac{\lambda_L^0}{1 + \dfrac{m}{(1 + hm)} \dfrac{L}{P} \left(\dfrac{dP}{dL} \right)}.$$ (9)

2.2. Definitions of Gains and Feedback Factors

In the presence of a feedback, the gain of the system, G_L, is the response with the feedback divided by the response without the feedback:

$$G_L = \frac{\Delta L}{\Delta L_0} = \frac{\lambda_L}{\lambda_L^0} = \frac{1}{1 + \dfrac{m}{(1 + hm)} \dfrac{L}{P} \left(\dfrac{dP}{dL} \right)} . \tag{10}$$

If $G_L < 1$, the inclusion of the feedback has damped the response of the system (that is, a negative feedback). If $G_L > 1$ the response of the system has been amplified (that is, a positive feedback).

It is also useful to define a feedback factor, f_L, by the relationship $G_L = 1/(1 - f_L)$. It can be shown that the feedback factor is proportional to the fraction of the system output that is fed back into the system input, so defining the feedback interaction (Roe, Feedbacks, timescales, and seeing red, unpublished manuscript). $f_L < 0$ means $G_L < 1$ and so reflects a negative feedback. $0 < f_L < 1$ means $G_L > 1$ and a positive feedback. If $f_L \geq 1$, the gain is undefined—the positive feedback is sufficiently strong that no equilibrium state can be established and unconstrained runaway growth is implied. As will be seen in Section 6, one advantage of defining feedbacks factors is that when more than one feedback is present, the individual feedbacks factors can be summed to give the overall system gain via: $G_L = 1/(1 - \Sigma_i f_{L_i})$. In contrast the individual gains cannot be summed (Roe, Feedbacks, timescales, and seeing red, unpublished manuscript). It should also be noted that feedback factors and gains characterize the change from one equilibrium state to another. Since those equilibrium states are governed by the surface geometry of the orogen and the model assumptions, the presence of a crustal root for the orogen does not change the strength of the feedbacks. It does however affect the time dependent behavior of the system, as shown in Section 8.

So from (10), in this case the feedback factor is given by

$$f_L = -\frac{m}{(1 + hm)} \frac{L}{P} \frac{dP}{dL} . \tag{11}$$

It can be seen from (11) that the sign of the feedback depends only on the sign of dP/dL. If $dP/dL > 0$, an increase in wedge size also increases the precipitation. This increases the erosional flux, which opposes growth of the wedge (provided those sediments are not recycled—see Section 6.3), and so the feedback is negative (that is, $f_L < 0$). Conversely, if $dP/dL < 0$ then $f_L > 0$: the feedback is positive, and the interaction of the orogen with the precipitation results in a larger wedge.

An important point is that P appears in both the numerator and denominator in (11). This means that the size of the feedback depends only on the functional form of $P(L)$ and not on its magnitude. Finally, the magnitude of f_L increases with m. This makes sense as m is the exponent on discharge in the erosion law, and so a larger value places more emphasis on discharge and precipitation.

3. OROGRAPHIC PRECIPITATION

The presence of topography influences climate across an enormous range of spatial scales (see Smith, 1979; Roe, 2005; Smith, 2006 for reviews). The Tibetan Plateau and the Rockies are large enough to affect the global-scale atmospheric circulation (for example, Smith, 1979), but even individual ridges and valleys (at the scale of a few kms) impact a host of meteorological factors (for example, Blumen, 1990), including the pattern of precipitation (Anders and others, 2007). In keeping with the approach of this paper, we focus on climate patterns at the scale of small, frictional orogens, and in particular, on the well-known case of a rain-shadow. Where the axis of an orogen lies perpendicular to the prevailing wind direction there is predominant ascent of the air on the windward flank. The resulting adiabatic expansion, cooling, and saturation of the air enhances the precipitation. Predominant

descent of the air to the lee suppresses precipitation there. In the case of the Southern Alps in New Zealand for example, precipitation rates exceed 10 m yr^{-1} on the windward flank, while dropping to less than 1 m yr^{-1} in the lee. In the Olympic mountains of Washington State, the respective values are 5 m yr^{-1} and 0.7 m yr^{-1} (for example, Wratt and others, 2000; Anders and others, 2007).

The orographic precipitation model we use is that of Roe and Baker (2006), and is shown schematically in figure 2. It has parameterizations of the conversion of cloud water into precipitation particles, and of the finite fall speed of those particles. Advection by the prevailing wind means that the precipitation is smoothed and displaced downwind from the condensation region. It is obviously highly-simplified and is intended to provide only the qualitative tendency of how orographic precipitation changes as a function of orogen size and prevailing wind direction. Its virtue is its simplicity and analytical tractability. Recalling that the purpose of this study is to understand the essential character of the orogen dynamics, a simplified and reduced model of orographic precipitation is the appropriate tool to use.

Here we give a brief review of the orographic precipitation model, as a much more comprehensive description of the model and its performance across a wide range of model parameters is given in Roe and Baker (2006). The model assumes a saturated column of air, u, impinging on a wedge-shaped orogen. The height of the orogen is H, the windward and leeward widths are L_W and L_L respectively. To a good approximation, the moisture content of a saturated atmosphere decreases exponentially with height, with an e-folding scale of H_m (for example, Roe, 2005). H_m varies with latitude, and is about 4 km in the tropics, and 2 km in high latitudes. On encountering the orography, the airflow is assumed to ascend uniformly at all levels with a vertical velocity equal to the mechanically-forced lifting at the surface ($w = uH/L_W$). This assumption neglects the dynamical response of the airflow to orography, an aspect which is captured in the model of Smith and Barstad (2004). Because the impinging air is saturated, wherever there is lifting there is also condensation. The condensation occurring at altitude reaches the ground only after cloud droplets are converted to hydrometeors (that is, rain or snow), and only after those hydrometeors have fallen to the ground. We assume that a finite period of time, τ_g, must elapse for the growth of cloud droplets to form hydrometeors, and that thereafter they fall with a characteristic terminal velocity, v_f. In essence this assumes a single representative size scale for
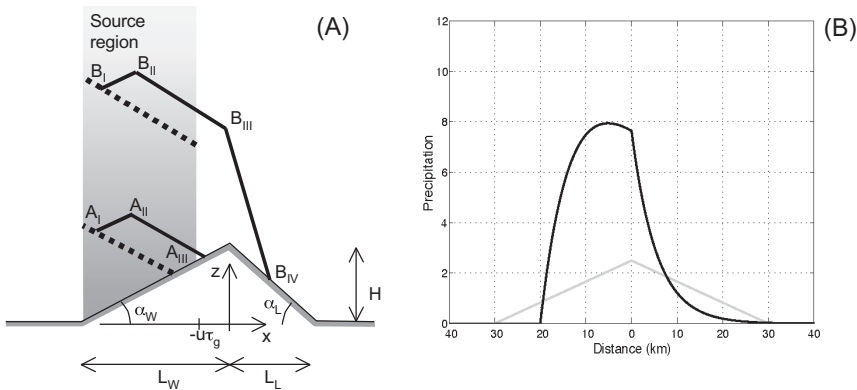

Fig. 2. (A) Schematic illustration of orographic precipitation model. Black lines are precipitation trajectories. The dashed lines are source lines that delineate all points within the source region where condensation ends up as precipitation at the same surface point. (B) Distribution of precipitation across the orogen for typical parameters. Units are arbitrary. See text for more details.

hydrometeors, and so neglects any size distribution. Collection or coalescence of cloud water droplets on the way down is also not treated explicitly, and so the changes in the trajectories that this mass accumulation results in are not included either.

These assumptions give the following characteristic 'pathways', or trajectories for the falling hydrometeors, depending on whether the precipitation ends up falling on the windward or leeward flanks of the range, illustrated in figure 2A.

For the windward flank:
- A_I to A_{II}: growth of droplets during which they are carried with the ascending flow.
- A_{II} to A_{III}: hydrometeors fall through ascending air.

For the leeward flank:
- B_I to B_{II}: as for A_I to A_{II}.
- B_{II} to B_{III}: as for A_{II} to A_{III}.
- B_{II} to B_{IV}: hydrometeors fall through descending air.

Finally, for $x_s > L_L$, the last part of the trajectory is through air with no vertical velocity.

These trajectories result in a "source region" on the windward flank. Because of the finite formation time for hydrometeors, it ends at $x = -u\tau_g$ (as indicated by fig. 2). The finite growth time also means that no precipitation reaches the ground for $x_s < -L_W + u\tau_g$. For every point on the surface downwind of this, a "source line" can be defined as the locus of points in the source region from which condensation ends up as precipitation at that surface point. Evaporation of falling precipitation into subsaturated air can also be incorporated, but for simplicity is neglected here. The precipitation reaching any given point on the ground is then given by the integral of the condensation rate along the source line for that point. Roe and Baker (2006) derive expressions for the precipitation pattern under these conditions. The expressions are simple enough to be integrated, and so can be used to calculate the average precipitation rates over the windward and leeward flanks. The equations nondimensionalize naturally by introducing four physically-meaningful parameters. Subscripts (W,L) denote windward and leeward sides respectively:

$$R_0 \equiv \frac{\rho_0 q_0 u H}{L_W}$$

Vertically-integrated condensation rate in a windward air column.

$$\theta_{W,L} \equiv \frac{L_{W,L} v_f}{u H}$$

The ratio of the raindrop trajectories slope to the orographic slopes.

$$\mu \equiv \frac{H}{H_m}$$

(12)

The ratio of mountain height to moisture scale height.

$$\psi_{W,L} \equiv \frac{L_{W,L}}{u \tau_g}$$

The ratio of mountain length to the formation length scale.

q_0 and ρ_0 are the saturation specific humidity and the density of air at $z = 0$. The equations for the average windward and leeward precipitation rates are:

$$P_W = \left(\frac{\theta_W}{\theta_W - 1}\right) \frac{R_0}{\mu} \left\{ 1 - exp\left[-\mu\left(1 - \frac{1}{\psi_W}\right)\right] - \frac{1}{\theta_W} + \frac{1}{\theta_W} exp\left[-\mu\theta_W\left(1 - \frac{1}{\psi_W}\right)\right]\right\} \quad (13)$$

$$P_L = \left(\frac{\theta_W}{\theta_W - 1}\right) \frac{R_0}{\theta_L \mu} \left\{1 - exp\left[-\mu\left(1 - \frac{1}{\psi_W}\right)(\theta_W - 1)\right]\right\} exp\left[-\mu\left(1 - \frac{1}{\psi_W}\right)\right]$$
$$\times [1 - exp(-\theta_L \mu)]. \quad (14)$$

In the limit of large orogen size and of steep trajectories of falling hydrometeors, $\psi_{W,L}, \theta_{W,L} \gg 1$, and the expressions above boil down to:

$$P_W = \frac{R_0}{\mu}(1 - e^{-\mu})$$

$$P_L = \frac{R_0}{\theta_L \mu} e^{-\mu}. \quad (15)$$

In this limit then, the average precipitation on the windward flank asymptotically approaches a constant value when the orogen height greatly exceeds the moisture scale height (that is, for $\mu \gg 1$), as it grows to intercept almost all of the impinging moisture flux. Correspondingly, the precipitation on leeward flank declines to zero.

3.1. Precipitation as a Function of Orogen Size

For the standard case used generating in figure 3, we use $u = 5$ ms^{-1}, $v_f = 4$ m s^{-1}, $\tau_g = 500$ s, $H_m = 3$ km, $q_0 = 4$ g kg^{-1}, $\rho_0 = 10^3$ kg m^{-3}. Following the terminology of Willett and others (1993), the pro-wedge is the flank of the orogen on the side from which material is being accreted, typically that of the subducting plate, and the retro-wedge is on the side of the overriding plate. In this paper, we assume a pro-wedge with a shallow topographic taper angle of 2° and a retro-wedge with a steeper topographic taper angle of 6°, similar to what is seen in Taiwan (Stolar and others, 2007b).

The average pro-wedge and retro-wedge precipitation rates produced by the Roe and Baker model as a function of total orogen width are shown in figure 3A, for the case where the pro-wedge is in the windward direction, and in figure 3B for the case where the pro-wedge is in the leeward direction. For small orogen widths, the advection of precipitation by the prevailing wind means that the windward and leeward
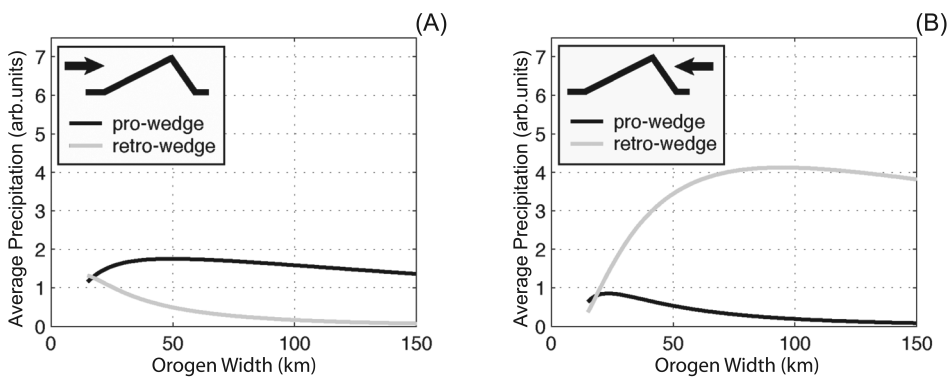

Fig. 3. Modeled average orographic precipitation rates on the pro-and retro-wedges as a function of total orogen width for the case of (A) windward pro-wedge, and (B) leeward pro-wedge case. The arrow in the legend indicates the prevailing wind direction. Note the switch in the wind direction switches the side receiving the most precipitation. The greatest precipitation rates occurs on steep, windward slopes. The precipitation rate units are arbitrary since the magnitude does not matter for the feedback. The pro-wedge taper is 2°, and the retro-wedge 6°, making the pro-wedge width about 75% of the total width. Details of orographic precipitation model and other parameters used are in Section 3.

flanks of the orogen receive roughly equal amounts of precipitation. As orogen width increases, the rain shadow deepens. For larger orogen widths, average precipitation rates on both flanks tend to decrease with orogen size because the vertically-averaged moisture content in the atmosphere decreases exponentially with surface height (for example, Roe, 2005). The highest average precipitation rates occur with a windward retro-wedge (as for the Southern Alps of New Zealand) because of the high rates of condensation there when ascent of the prevailing airflow occurs over the steep slope.

3.2. Discussion of Precipitation Model

The main reason for using this particular precipitation model is that, for a wedge-shaped orogen, it provides analytical expressions for the average windward and leeward precipitation rates in terms of only a few model parameters. There are many other simple models of orographic precipitation that are available, each with their strengths and weaknesses (for example, Roe, 2005; Smith, 2006). For the same topography different models can produce quite different patterns of precipitation. An alternative, the model of Smith and Barstad (2004), is straightforward to implement and also incorporates the dynamical response of the atmosphere to flow over orography. Using the Smith and Barstad model does not produce qualitatively different results from those presented here.

In many places, especially in midlatitude settings where the basic climate regime has not changed over millions of years, the persistence of a rain shadow can be taken for granted. However, the magnitude of that rain shadow and its variation over time are much less certain. No simple diagnostic model of orographic precipitation should be thought of as directly representing the real atmosphere (for example, Roe, 2005; Smith, 2006). The microphysical conversion processes operating within clouds are extremely complex and dependent on the details of the ambient conditions (for example, Riesner and others, 1998). The climatological distribution of precipitation is the average of many individual storms, each with their own varying temperatures and complex wind patterns. For example, neither the European Alps nor Taiwan have well-defined climatological rain shadows, even though substantial rain shadows do exist storm-by-storm. Moreover, both the frequency and intensity of storms are controlled by the much larger-scale general circulation of the atmosphere. On the time scales of orogen development, the influence of these global-scale circulation patterns on regional climates is highly uncertain (for example, Kageyama and others, 1999). Any effort to quantify the effect of precipitation feedbacks cannot circumvent these issues. In light of this, we regard the precipitation model used here as providing a physically-based rule for how precipitation rates might reasonably change with changing orogen size, in the simplifying case of all else remaining unchanged.

Lastly, in representing climate only in terms of a precipitation rate, we neglect the potentially very important role of episodic glaciations on the landscape. We comment further on this omission in the Discussion.

4. THE CASE OF A ONE-SIDED CRITICAL WEDGE OROGEN

To begin with we consider the case of a one-sided critical wedge, shown schematically in figure (4). The purpose of presenting the one-sided case is primarily didactic—it is the framework in which the basic behavior of the coupled system can be most clearly understood. The goal is to characterize the strength of the interactions among the climatic, erosional, and tectonic components of the system. This can be quantitatively addressed by calculating the system sensitivity and feedback and gain factors (as in Section 2). In Section 6 the analysis is generalized to a two-sided wedge with some recycling of sediment into the pro-wedge.
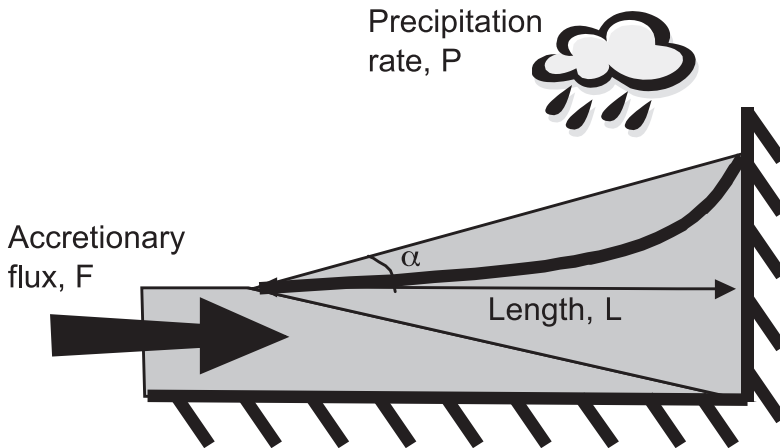
Fig. 4. Schematic illustration of model framework and parameters for the one-sided critical wedge. An accretionary flux incorporates new mass to the system. Fluvial erosion, represented here by a longitudinal profile of a river, removes mass. In steady-state the two fluxes balance.

4.1. Results of Coupling One-Sided Critical Wedge Orogen to Orographic Precipitation Model

The geometry of the critical wedge is the same as in Section 3. We set $h = 2$. The standard set of erosion parameters we use, $(m, n) = (1/2, 1)$, is predicted theoretically if fluvial erosion is proportional to unit stream power. We also present results for two other combinations: $(m, n) = (1, 2)$, and $(m, n) = (1/3, 2/3)$. Whipple and Tucker (1999) review the bases for these combinations. Average precipitation rates are calculated from (13) and (14), and characteristic parameters are given in Section 3.

We calculate the gains separately for the pro-and retro-wedges, treating them as uncoupled one-sided wedges, using (11), and for both possible wind directions. Figure 5 plots the one-sided gain factors against the wedge widths varying between 20 and 150 km. A gain of 50 percent means the precipitation feedback makes the wedge half as
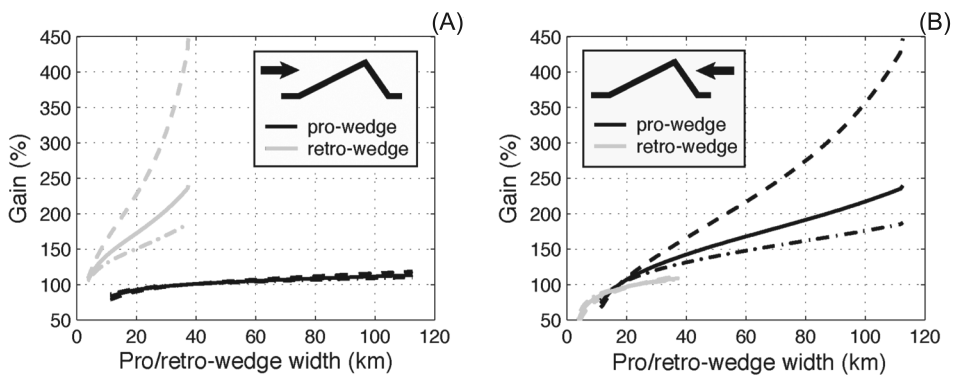

Fig. 5. Gains for pro-wedge (black lines) and retro-wedge (gray lines), for the case where the wedges are not coupled together (that is, they are treated as separate one-sided wedges). (A) windward pro-wedge case, (B) leeward pro-wedge case. The graph plots the gains as a function of the respective pro/retro-wdege widths. Line styles denote the value of erosion parameters. Dashed line, $(m, n) = (1, 2)$; Solid line, $(m, n) = (1/2, 1)$; and dash-dot, $(m, n) = (1/3, 2/3)$. The graphs show calculations for a total orogen width (that is, pro-wedge plus retro-wedge) ranging from 15 to 150 km. Other parameters are given in the text.

sensitive to changes in F, compared to no precipitation feedback. A gain of 200 percent means the sensitivity is doubled.

For both prevailing wind directions there is a strong positive feedback on the leeward wedge. The drying of the leeward wedge as the orogen grows (that is, $dP_L/dL < 0$, as seen in fig. 3) reduces erosion and amplifies changes in wedge size. The strength of the feedback depends quite sensitively on the value of the erosion parameters. As is clear also from (11), the larger the value of m, the stronger the feedback. For the case of $m = 1$ the gain reaches 450 percent.

The windward wedge shows a smaller range of gains ($\sim 50\%$ to $\sim 120\%$) as width varies, and not much variation for different erosion law parameters. This reflects the smaller variations in windward precipitation rates predicted by the orographic precipitation model (fig. 3). The smallest gain factor (of just over 50%) occurs for the case of a small, windward retro-wedge. This means a strong negative feedback factor of $f = -1$, and arises because of the significant increase of precipitation with orogen size (that is, $dP_W/dL > 0$, as seen in fig. 3). Increases in orogen size are strongly damped by the accompanying increases in precipitation and erosion.

Focusing on the windward flank of the orogen in figures 3A and 3B, there is a transition from $G < 100\%$ to $G > 100\%$ that occurs at about 40 km width in the pro-wedge case, and at about 20 km (fig. 3A) in the retro-wedge case (fig. 3B). This marks the point at which the feedback changes from negative to positive. From (11) it occurs when dP/dL changes sign, as also seen in figure 3 (though note the different axes). Physically, this happens because of the exponential decrease of atmospheric moisture content with height. As the orogen grows, the condensation rate generated by ascent of the air increases, but because of the limited moisture availability, it eventually asymptotically approaches a constant value. At some point during the orogen growth, the fact that this condensation rate is being distributed over a larger and larger width comes to dominate, and average precipitation rates then start to decrease with further orogen growth. The exact transition point from negative to positive feedback is dependent on our choice of critical taper and the precipitation model parameters, which are uncertain and variable. But nonetheless, that such a transition should exist is a confident expectation, and at this transition the feedback reverses sign.

4.2. Runaway Growth

An interesting though somewhat exotic possibility arises when $f_L \geq 1$. For equilibrium orogen to exist there must be a balance between accretionary flux and total erosional yield from the orogen [(7) implicitly assumes that such an equilibrium is possible]. If $dP/dL = 0$, then from (1), erosional yield varies as $L^{(1+hm)}$ and thus increases with orogen size. Therefore an increase in accretionary flux, which tends to increase orogen size, can be balanced by the accompanying increase in erosional yield. However if dP/dL is sufficiently negative it can overcome this natural tendency: the erosional yield cannot come into balance with the increased accretionary flux and there follows unstable runaway growth of the wedge.

From (11) and (5), $f_L \geq 1$ requires that

$$\frac{dP}{dL} \leq -\frac{(1 + hm)}{m}\frac{P}{L}. \tag{16}$$

For the moment, we keep to the case of one-sided wedge cases. The effects of coupling the two wedges are presented in the next section. (15) gives the expression for precipitation in the limit of a large orogen and steeply-sloping precipitation trajectories. For the windward precipitation rate at large orogen widths, it can be

shown that the feedback factor asymptotically approaches a constant value of $f_L = m/(1 + hm)$. (16) is never satisfied, and so the wedge is always stable.

However, for the leeward precipitation rate, the feedback factor is equal to

$$f_L = \frac{m}{(1 + hm)}(1 + \mu),\tag{17}$$

Since $\mu \equiv H/H_m$, (16) can be satisfied if

$$H > \frac{(1 + hm - m)}{m} H_m.\tag{18}$$

H_m varies with latitude, ranging from ~2 km in the high latitudes to ~4 km in tropics (for example, Roe, 2005). Taking $h = 2$ and common values for m of 1, 1/2, and 1/3, (18) predicts runaway growth for $H > 2H_m$, $3H_m$, and $4H_m$, respectively.

The predicted orogen sizes for which runaway growth could occur are large compared to mountain ranges on Earth. It should be noted though, that with a formulation of the erosion law that is more sensitive to discharge, particularly one with threshold stress or discharge (for example, Costa and O'Conner, 1995; Tucker and Bras, 2000), runaway growth might occur for significantly smaller (and more realistic) orogen sizes.

The possibility of unconstrained growth is an interesting idealization. However in the presence of such a strong positive feedback eventually, of course, some other process such as glaciation at high elevations, or thermal weakening of the brittle crustal root would come about. It is important to emphasize that the self-similarity assumption of the critical wedge model will increasingly break down beyond some orogen height. As the crust thickens the resulting increase in basal temperature will produce increasingly viscous deformation, after which point the orogen height will asymptotically approach the mechanical limit, and a plateau will form (for example, Willett, 1999b; Roe and Brandon, Critical form and feedbacks in mountain belt dynamics: the role of rheology as a tectonic governor, unpublished manuscript). The runaway condition presented here is perhaps best thought as a sufficient (but not necessary) condition for plateau formation. That is, the plateau condition can be reached in less extreme circumstances than lead to a predicted runaway via the precipitation feedback.

5. RESPONSE OF ROCK UPLIFT RATES TO THE PRECIPITATION FEEDBACK

In steady state the rock uplift rate is equal to the vertical component of the exhumation rate, which, through thermochronometry is potentially an observable indicator of the dynamics of an active orogen (for example, Reiners and Brandon, 2006). This is one reason it is useful to explore how the rock uplift rate depends on the strength of the precipitation feedback. This section also illustrates that the interpretation of the strength and even the sign of the feedbacks depends on which variable is declared to be of interest, and on the choices made in defining feedbacks. These points are dwelt on in more detail in Roe (Feedbacks, timescales, and seeing red, unpublished manuscript).

Again, to begin with, we present analyses for the uncoupled, one-sided wedges. For convenience we can assume a uniform rock uplift rate (in the two-sided case, it will be different in the pro-and retro-wedges). Roe and others (2006) and Stolar and others (2006, 2007a) showed that the spatial pattern of rock uplift rates across the orogen does not change the system scaling relationship [that is, (1)], nor does the difference between the one-sided and two-sided cases matter (Appendix A). Of course, the material trajectories through the orogen system do depend on the relative importance of underplating and frontal accretion (for example, Brandon and others, 1998;

Whipple and Meade, 2004; Stolar and others, 2005). A simple requirement of mass balance in steady-state means that the trajectories must adjust such that the patterns of fluxes into the system (that is, underplating, frontal accretion, and erosion) are balanced, and for an incompressible material there is a unique solution (for example, Brandon and others, 1998; Stolar and others, 2005, 2007a). This means that for a true Coulomb plastic material the internal mechanics of how the deformation occurs does not matter for the purpose of understanding the system sensitivity, at least as it is defined in Section 2. Roe and Brandon (Critical form and feedbacks in mountain belt dynamics: The role of rheology as a tectonic governor, unpublished manuscript) find that this is also a good approximation for a viscously-deforming material.

A rock uplift sensitivity factor can be defined in an analogous way to the width sensitivity factor:

$$\Delta U = \lambda_U \Delta F, \tag{19}$$

where the subscript U denotes rock uplift. Since $F = U \cdot L$, we can write

$$\frac{\Delta F}{F} = \frac{\Delta U}{U} + \frac{\Delta L}{L}$$
$$= \frac{\Delta U}{U} + \frac{\lambda_L}{L} \Delta F, \tag{20}$$

and therefore

$$\lambda_U = \frac{F}{L}\left(\frac{1}{F} - \frac{\lambda_L}{L}\right). \tag{21}$$

(21) is a general expression that applies whether there is a precipitation feedback or not. For the no feedback case, substitution from (5) gives

$$\lambda_U^0 = \frac{1}{L} \frac{hm}{(1 + hm)}. \tag{22}$$

In comparison with (5), the rock uplift sensitivity factor is somewhat less dependent on the value of the parameters h and m than the width sensitivity factor.

Also using (5) and (21) the rock uplift gain can be written as

$$G_U = \frac{1 + hm - G_L}{hm}. \tag{23}$$

An important trade-off between orogen width and rock uplift occurs as the system establishes a new equilibrium. This is evident from the relative sign difference between λ_L and λ_U in (21) and between G_L and G_U in (23): a high sensitivity of width to accretionary flux means a low sensitivity of rock uplift rates. For a specified increase in accretionary flux, a higher width sensitivity means the additional accretionary flux is distributed over a larger width. Therefore the local rock uplift rates are proportionately less than if the additional flux had to be accommodated over a smaller width.

If G_L is sufficiently large it is even possible for G_U to be negative: that is, an increase in accretionary flux leads to a decrease in rock uplift rates. This counterintuitive result occurs in the case of a strongly positive precipitation feedback. For a given increase in accretionary flux, a sufficiently strong positive feedback can mean the orogen width increases by so much that the local rock uplift rate is actually reduced. Using (23), it can be calculated from the curves in figure 5 that this is in fact happening for the leeward retro-wedges exceeding ~30 km, and leeward pro-wedges exceeding ~90 km.

6. THE CASE OF A TWO-SIDED CRITICAL WEDGE OROGEN

The feedback framework developed in the last section can be generalized to a two-sided wedge with sediment recycling (Whipple and Meade, 2004), a schematic of which is shown in figure (6). In the derivations below, all variables have the same meaning as in Section 2.2, but the subscripts p and r are used to denote properties that apply to the pro-and retro-wedges respectively. Following Whipple and Meade (2004), we also allow for a fraction of the material eroded off the pro-wedge, ξF_p, to be reincorporated into the orogen.

To start with, the pro-and retro-wedge each must satisfy their own scaling relationship:

$$F_p = \eta_p K_p L_p^{1+hm} P_p^m$$

$$F_r = \eta_r K_r L_r^{1+hm} P_r^m. \tag{24}$$

where we have now explicitly retained the rock erodibility, K, in the scaling relationship (for example, Roe and others, 2006). The requirement that the wedges are coupled produces two constraints that make the problem tractable. Firstly, in equilibrium the fluxes accommodated under the pro-and retro-wedges must sum to the total incoming flux, so conservation of mass implies

$$F = (1 - \xi)F_p + F_r. \tag{25}$$

In the limit of complete recycling of sediment on the pro-wedge therefore, all the fresh accretionary flux must be accommodated within the retro-wedge (Whipple and Meade, 2004).

Secondly, the constraint that both wedges have the same height means

$$L_p \tan \alpha_p = L_r \tan \alpha_r, \tag{26}$$

and the total width of the orogen is thus given by $L = L_p + L_r$. We first present how the precipitation feedback affects the partitioning of rock uplift rates between the two flanks of the orogen, and then derive expressions for the gain and feedback factors.
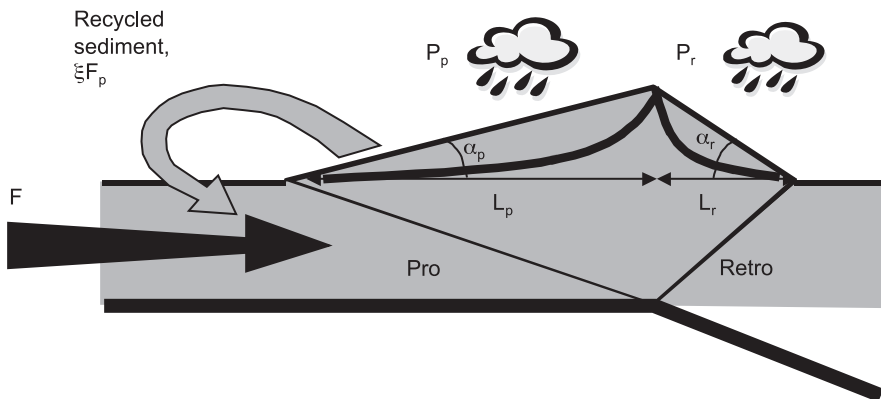

Fig. 6. Schematic illustration of the model framework and parameters for the two-sided critical wedge. A fraction of the material eroded off the pro-wedge is recycled back into the pro-wedge.

6.1. Partitioning of Rock Uplift Rates

All of the accretionary flux must get apportioned into the pro-and retro-wedges. The resulting rock uplift rates reflect both the partitioning of this flux and the relative width of each wedge. The rock uplift rates also depend on the erosion on each wedge, and therefore on the precipitation.

Whipple and Meade (2004) used the pro-and retro-scaling relationships to derive expressions for the ratio of rock uplift rates on pro-and retro-wedges. We can write $U_p = F_p/L_p$ and $U_r = F_r/L_r$, and then from (24) and (26) the ratio of the rock uplift rates can be written as

$$\frac{U_p}{U_r} = \left(\frac{\eta_p/(\tan \alpha_p)^{hm}}{\eta_r/(\tan \alpha_r)^{hm}} \right) \left(\frac{P_p}{P_r} \right)^m \frac{K_p}{K_r}. \tag{27}$$

Note that the ratio of rock uplift rates does not depend on the fraction of sediment recycling. In general η_p and η_r are implicit functions of the model geometry and parameters, including the critical taper angles (Roe and others, 2006). Note, however, that the quantity $\eta/(\tan\alpha)^{hm}$ always increases with taper angle. Therefore, for uniform erodibility and no rain shadow (that is, $K_p = K_r$, $P_p = P_r$), the rock uplift rate is always larger on the retro-wedge than on the pro-wedge. Taking $\alpha_p = 2°$ and $\alpha_r = 6°$, and typical choices of model parameters, (27) predicts the rock uplift rate is greater on the retro-side by between 2 percent and 25 percent (see also Whipple and Meade, 2004). In the case of non-uniform erodibility (that is, $K_p \neq K_r$), the rock uplift rates are preferentially focussed towards the more erodible flank.

For fixed wedge geometry and model parameters, (27) also shows that the partitioning of rock uplift rates is proportional to the ratio of the precipitation rates, raised to the power m. If the precipitation rate on one wedge is low, less erosion occurs there. Consequently more accretionary flux must be accommodated within the other wedge, enhancing the rock uplift rate there. For common choices of model parameters, $1/3 \leq m \leq 1$, and so the ratio of the rock uplift rates is somewhat damped relative to the ratio of the precipitation rates.

The ratio of rock uplift rates calculated from (27), (13), (14), and assuming $K_p = K_r$ is shown in figure 7. For small orogens, $P_W \sim P_L$, and so $U_r > U_p$. For most of the orogen widths considered though, rock uplift rates are strongly focused onto the wet, windward flank of the orogen. For an orogen with a width of 100 km, and the case of a windward prowedge, rock uplift rates are about two-and-a-half times larger on the windward flank. In the case of a windward retro-wedge, rock uplift rates are about five times higher.

While it should be noted that the comparison of rock uplift rates and exhumation rates is complicated by the horizontal advection of material within the orogen (for example, Stolar and others, 2005), observations (for example, Tippet and Kamp, 1993; Brandon and others, 1998) and numerical models (for example, Willett, 1999a) suggest that the partitioning of exhumation rates between pro-and retro-wedges depends sensitively on the prevailing wind direction, as predicted by our model.

6.2. Response of Two-Sided Orogen to a Climate Feedback

In Appendix A, it is shown that the width sensitivity factor without a climate feedback, λ_0, is the same for the two-sided wedge as for the one-sided wedge [that is, (5)]. A derivation is also given for the gain, G_L, of the two-sided wedge with a precipitation feedback:

$$G_L = \frac{1}{1 + m\lambda_L^0 \left[(1 - \xi) \frac{F_p}{P_p} \frac{\partial P_p}{\partial L} + \frac{F_r}{P_r} \frac{\partial P_r}{\partial L} \right]}. \tag{28}$$
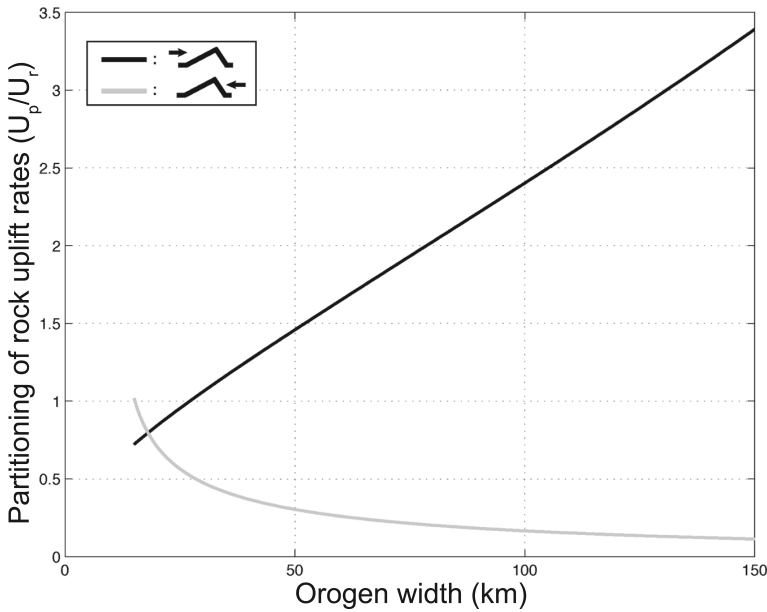
Fig. 7. The curves plot the ratio of rock uplift rates on the pro-and retro-wedges as a function of orogen size, for two cases: the black line shows the case where the pro-wedge is also the windward flank, and the gray line shows the case where it is the retro-wedge that is the windward flank. The graph therefore shows that rock uplift is strongly focused on the windward flank of the orogen. In both cases, the drying of the leeward flank as the orogen grows means rock uplift rates are reduced there, so favoring greater rock uplift on the windward side. Without a precipitation feedback the partitioning of rock uplift rates would not vary with orogen width. In the legend the arrow indicates prevailing wind direction.

The strength of the precipitation feedback depends, therefore, on how the pro-and retro-precipitation changes as a function of orogen size (that is, on $\partial P_p/\partial L$ and $\partial P_r/\partial L$), the magnitude of the fluxes, and the amplitude of the precipitation rates.

By analogy with (10) and (11), the last two terms in the denominator of (28) can be thought of as separate feedback factors, f_p and f_r, governing the individual (though now coupled) responses of the pro-and retro-wedges:

$$f_p = -(1 - \xi)m\lambda_L^0 \frac{F_p}{P_p} \frac{\partial P_p}{\partial L}$$

$$f_r = -m\lambda_L^0 \frac{F_r}{P_r} \frac{\partial P_r}{\partial L}. \tag{29}$$

Since f_p and f_r do not necessarily have the same sign, there can be a trade-off between the pro-and retro-wedge feedbacks. Also (29) shows that the higher the fraction of sediment recycling, the less the pro-wedge is able to accommodate the unrecycled flux, and so the less important it is in determining the response of the combined system.

The terms in (28) can be computed from (24), (25), (27), (13) and (14). Figure 8 shows the gain of the two-sided wedge, as a function of total width. For comparison, the gains for the individual, uncoupled pro-and retro-wedges are also shown. The gain of the combined system always lies in between gains of the individual pro-and retro-wedges. Thus, as might be expected, the two-sided system strikes a compromise between the sensitivities of the separate one-sided wedges. To begin with, imagine two
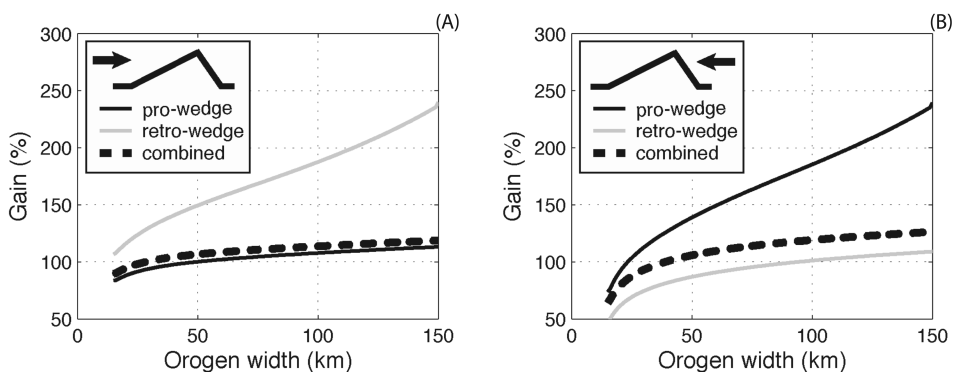
Fig. 8. Uncoupled pro-wedge gain, uncoupled retro-wedge gain, and fully-coupled two-sided wedge gain, plotted as a function of total orogen width (note the different scale from fig. 5), for (A) windward pro-wedge case, (B) leeward pro-wedge case. There is no recycling of sediment. The windward flank of the orogen tends to dominate the overall sensitivity of the system. In the legend the arrow indicates the prevailing wind direction.

uncoupled, one-sided wedges. The wedge with the higher gain is more sensitive and so requires a bigger change in width to accommodate a given change in flux. When the two wedges are now coupled together, some of that extra material can be accommodated through the lower gain wedge, and so a lower overall response results. Conversely, from the perspective of the lower gain wedge, its coupling to the more sensitive, higher gain wedge forces it to have larger width changes than would be the case in the uncoupled situation.

Figures 8A and 8B show that the overall gain of the system does tend to lie close to the gain of the windward flank of the orogen (be it the pro-or retro-wedge). Physically, the gain is a measure of how the coupling to precipitation affects the adjustment to an increase in accretionary flux. As shown in figure 7, in the case of a strong rain shadow without recycling, the orogen accommodates much the greater proportion of the new material within the wet, windward flank where erosion rates are already high, than through the dry, leeward flank where erosion rates are low. Hence the sensitivity of the combined system is governed mainly by the adjustment of that windward flank.

Because the leeward flank of the orogen makes only a limited contribution to the gain of the coupled, two-sided system, the strong positive feedback predicted for the uncoupled, one-sided leeward wedge (that is, the gains shown in fig. 5) is significantly stabilized. The limited role played by the leeward flank is biggest if it is also the pro-wedge: the larger width of the pro-wedge means it accommodates a greater proportion of changes in accretionary flux (comparing figs. 8A and 8B). As is shown below, an exception to this result is when there is a high proportion of sediment recycling on the pro-wedge.

6.3. The Effect of Sediment Recycling

If some of the sediment eroded off the pro-wedge gets reincorporated into it [for example, $\xi > 0$ in (25)] through accretion of foreland sediments, the pro-wedge is less able to participate in accommodating the fresh, un-recycled portion of the accretionary flux (Whipple and Meade, 2004). In the limit of complete sediment recycling (that is, $\xi = 1$) the sensitivity of the system to changes in the far-field accretionary flux will be completely governed by the retro-wedge.

Figure 9 shows the gain of the system as a function of ξ, for an orogen of width 100 km. In the case that the pro-wedge is the windward flank of the orogen, it dominates
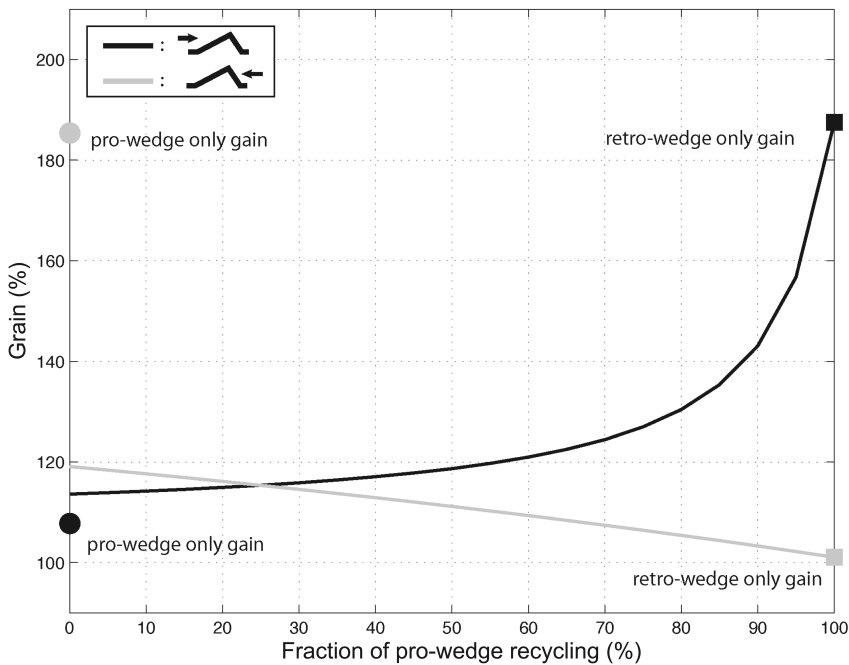
Fig. 9. The curves show the gain as a function of the percentage of sediment recycling on the pro-wedge for the windward pro-wedge and leeward pro-wedge cases, and for an orogen of total width 100 km. Also shown at 0% and 100% as circles and squares, respectively, are the individual pro-and retro-wedge gains for the two cases. When there is 100% recycling on the pro-wedge the system gain reduces to that of the retro-wedge. In the legend the arrow indicates the prevailing wind direction.

the sensitivity of the combined system at low recycling fractions (as seen also in fig. 8). Even with a substantial fraction of recycling, it continues to play an important role, because of its larger width than the retro-wedge. It is not until recycling reaches around 90 percent that the gain of the combined system becomes closer to the retro-wedge gain than to the pro-wedge gain. Conversely, in the case of a windward retro-wedge, the gain of the combined system is already strongly controlled by wet retro-wedge. Increasing the recycling on the pro-wedge only increases the importance of the retro-wedge, and consequently there is relatively little change in the system gain as ξ varies.

7. THE RELATIVE STRENGTH OF THE TECTONIC AND PRECIPITATION FEEDBACKS

It was noted in the introduction that the self-similar form of a critical wedge orogen can be interpreted as a strong negative feedback, and so a natural comparison to make is between the relative strengths of the precipitation and tectonic feedbacks. However, in order to do this, a slightly different definition of the precipitation feedback must be used. The reason is that feedbacks are only formally defined relative to a reference system (that is, a system without the interaction that produces the feedback, for example, Roe, Feedbacks, timescales, and seeing red, unpublished manuscript). Therefore in order to properly compare two feedbacks the same reference system must be specified.

We have defined the precipitation feedback relative to the critical wedge system because it is most natural to do so. However the critical wedge system obviously already includes the tectonic interaction. If the reference system is instead taken to be an

orogen of fixed-width, the direct comparison can be made. In the fixed-width reference system the tectonic feedback arises because L varies with H, and the precipitation feedback arises because P varies with H (H/L is the topographic slope the air must ascend or descend). Switching to this reference system does not change the typical magnitude of the precipitation feedbacks very significantly, and we note that the results are the same for one-sided and two-sided orogens.

For a fixed-width orogen (and fluvial erosion) the height, H, is given by

$$H \propto F^{1/n} L^{1/n} P^{-m/n}, \tag{30}$$

(for example, Whipple and others, 1999; Roe and others, 2006), and where the substitution $U = F/L$ has been used. The gain of the system can now be expressed in terms of the height change with and without the feedbacks (that is, $G = \Delta H/\Delta H_0$).

Following the same procedure outlined in Section 4, the gain for the fixed-width orogen can be expressed as

$$G = \frac{1}{1 - f^P - f^T}, \tag{31}$$

where f^P is the precipitation feedback factor given by

$$f^P = -\left(\frac{m}{n}\right)\frac{H}{P}\frac{dP}{dH}, \tag{32}$$

and f^T is the tectonic feedback factor given by

$$f^T = -\frac{1}{n}\frac{H}{L}\frac{dL}{dH}, \tag{33}$$

which for constant taper angle is just equal to $-1/n$. For the three values of n we consider, therefore, the tectonic feedback has a strong negative feedback factor of -1, -3/2, or -1/2, and is independent of H. f^P can be calculated as a function of H for the windward and leeward flanks from (13) and (14), and are shown in figure 10 for a range of orogen heights. The magnitude of the tectonic feedback is larger than the precipitation feedback, and except in the case of $n = 2$, more than twice as large. The interpretation of these results is that the tectonic requirement of self-similar form exerts a stronger control on the size of the orogen than does orographic precipitation.

8. THE CONNECTION BETWEEN FEEDBACK STRENGTH AND THE OROGEN RESPONSE TIME

So far, we have only considered orogens in steady state. Growth or decay of the orogen will occur if there is an imbalance between the accretionary flux and the erosional flux, $E(t)$. In the two-dimensional framework here, the rate of growth of the cross-sectional area, A, is the difference between the two fluxes:

$$\frac{\partial A}{\partial t} = F - E(t). \tag{34}$$

From the geometry in figure 6, $A = DL/2$, where D is the total thickness of the wedge, including the crustal root. For a requirement of local isostatic balance $D = H/(1 - \rho_c/\rho_m)$, where ρ_c and ρ_m are the crust and mantle densities, respectively. Expressing the cross-sectional area in terms of the wedge width and the pro- and retro- wedge angles gives:
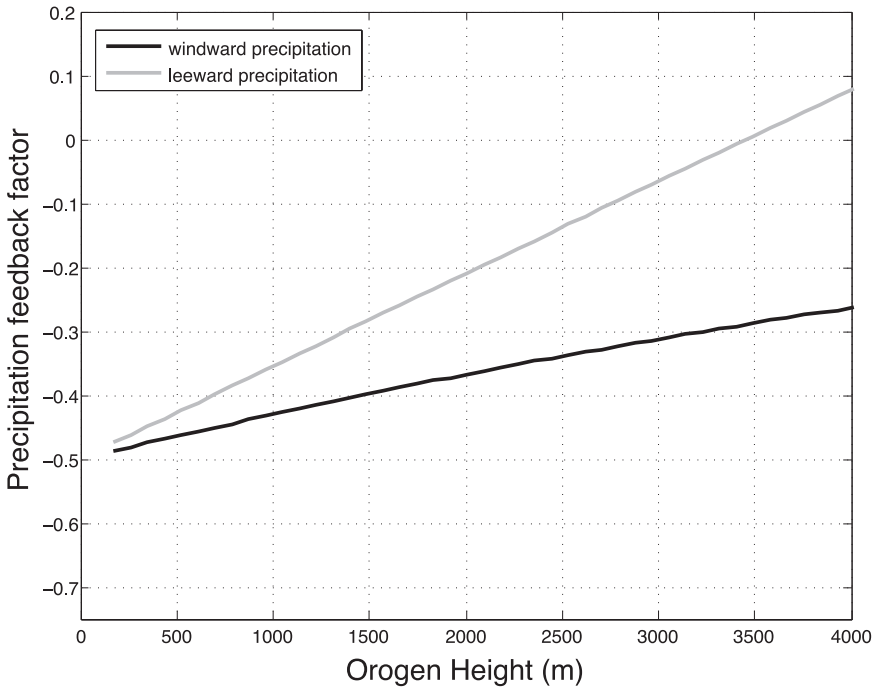
Fig. 10. Precipitation feedback factor calculated from (32), for windward and leeward precipitation, as a function of orogen height. $m/n = 1/2$, which applies for all combinations of (m, n) considered. For comparison, the equivalent tectonic feedback factor is -1, -3/2, or -1/2 for the different choices of n, and is independent of H. An orogen width of 50 km was used for this figure, although the curves are not sensitive to this choice.

$$A = \frac{1}{2(1 - \rho_c/\rho_m)} \frac{\tan \alpha_c \tan \alpha_r}{(\tan \alpha_c + \tan \alpha_r)} L^2. \tag{35}$$

Whipple and Meade (2006) studied this time dependent problem, and made the assumption that the orogen was at each instant in a quasi-equilibrium. That is, the wedge conforms to the self-similar form as it evolves through time, and not just at equilibrium. This means the erosional flux as a function of L and P will also follow the scaling relationship [that is, (1)]. Support for this assumption being valid on times scales relevant for orogen evolution comes from the numerical modeling results of Stolar and others (2006).

Consider the case of no initial topography and a sudden switching on of an accretionary flux, F_0. In the early stages of growth $F_0 \gg E$, and so from (34) the cross-sectional area of the orogen will grow approximately linearly with time. The orogen width will thus grow as the square root of time (see also Whipple and Meade, 2006).

When the orogen nears equilibrium the accretionary and erosional fluxes will be similar and so we can consider the linearized response of the system. Let $E(t) = F_0 - F_0(t)$, where F_0 is the flux imbalance. Similarly let $A = A_0 + A'$, where A_0 is the cross sectional area in equilibrium with F_0, and A' is the anomaly. The linearized form of (34) is then:

$$\frac{\partial A'}{\partial t} = -F' = -\frac{dF}{dA}\bigg|_{F_0} A', \tag{36}$$

which can also be written as

$$\frac{\partial A'}{\partial t} = - \frac{A'}{\left.\dfrac{dL}{dF}\right|_{F_0} \times \left.\dfrac{dA}{dL}\right|_{F_0}} .$$ (37)

The denominator on the right hand side of (37) has units of time and can be interpreted as the e-folding response time of the orogen. Noting that dL/dF is the sensitivity factor, λ, and using (35), this time scale can be expressed as

$$\tau = \lambda \frac{L}{(1 - \rho_c/\rho_m)} \frac{\tan \alpha_p \tan \alpha_r}{(\tan \alpha_p + \tan \alpha_r)} .$$ (38)

Defined in this way, the response time is proportional to the system sensitivity and also to the orogen size. (38) is a general expression that applies whether there is a precipitation feedback or not. Hence the ratio of the response times with and without a precipitation feedback, τ/τ_0, is equal to λ/λ_0, or in other words the gain of the system. Thus, the effect of the climate feedback on the response time of the orogen can be inferred directly from the gain curves plotted in figure (8).

Note that the response time defined here is a measure of the instantaneous rate of adjustment, so it is not the same thing as the total time taken to reach equilibrium, which would depend on the integrated history of the orogen development. However, using the expression for λ from (5) and the three common combinations of parameters given in Section 4.1, it can be shown that the dependency of τ on L is quite weak, and so a single characteristic value could be applied over a wide range of orogen sizes (for a similar conclusion from an independent analysis see also Whipple and Meade, 2006). Roe (Feedbacks, timescales, and seeing red, unpublished manuscript) discusses the general relationships between feedbacks and system response times in more detail than is done here.

9. SUMMARY

We have presented a very simple and reduced model of what, in reality, is an extremely complicated system. Orogenesis depends on myriad physical processes, from the rheology of rock deformation, to abrasion and plucking in turbulent river flows, to micron-scale cloud physics, and moreover, on their integrated histories over millions of years. It is probably unrealistic to expect that the individual processes, let alone their interactions, will ever be known well enough that models of orogenesis can be thought of as predictive simulations in, say, the same way that numerical weather forecasts are.

The alternative approach is to try to identify robust physical 'principles' that, under idealized conditions, the system will tend to obey. The consequences of combining these principles in a self-consistent way can be explored, and used to place bounds on the strength of their interactions. The three components of the system presented here: a self-similar critical topographic form; the discharge and slope dependence of fluvial erosion; and the development of a rain shadow, are probably best thought of as being principles in the sense indicated above.

The tendency of a critical-wedge orogen to maintain a self-similar topographic form as it grows or decays means that changes in local rock-uplift rates tend to oppose changes in tectonic or climatic forcing, and so strongly damp changes in orogen size. There is a trade-off between width changes and rock-uplift changes. For a given accretionary flux, an increase in width will produce a decrease in rock-uplift rate since the same accretionary flux is distributed over a larger area. A small sensitivity of orogen width implies a large sensitivity of rock-uplift rates.

The constraint of self-similar growth can be conceived of as a 'tectonic governor' (for example, Maxwell, 1868) that acts to strongly regulate the system response to changes in climatic or tectonic forcing. In a companion paper (Roe and Brandon, Critical form and feedbacks in mountain belt dynamics: the role of rheology as a tectonic governor, unpublished manuscript) it is shown that this regulatory effect is strong even if the deformation is more viscous: provided there is some tendency for deformation to act to restore the orogen shape in response to erosional unloading, the tectonic governor effect dominates the system dynamics.

If precipitation increases with orogen size, local erosion rates also increase. This damps the width changes, and the feedback is negative. Conversely if precipitation decreases with orogen size, width changes are amplified, and the feedback is positive. For the model developed here, the size of the feedbacks depend strongly on the parameters of the fluvial erosion law. At a general level, this demonstrates that the strength of the interactions depends strongly on the physics of erosion, and highlights how inextricably intertwined is the orogenic system. The size of the feedback also depends on the size of the orogen. It does not, however, depend on the magnitude of the precipitation rates, but only the functional form of its variation with orogen size. In the large orogen limit, the positive feedback can be such that the erosional flux is unable to balance the accretionary flux, and unconstrained runaway growth is predicted. It is intriguing to speculate on the role this strong positive feedback plays in plateau development: the operation of a positive feedback in nature would increase the likelihood that a given collisional orogen would eventually become a plateau, and also act to accelerate its development.

An increase in accretionary flux will tend to produce an increase in orogen width and an increase in rock uplift rates. The exception to this is the case of a strong positive precipitation feedback, which can cause such a large increase in width that rock uplift rates are actually reduced. This possibility complicates the observational test to discriminate between tectonically-or climatically-induced changes proposed by Roe and others (2006) and Whipple and Meade (2006).

In the two-sided critical-wedge orogen, the rain shadow has a dramatic impact on the partitioning of rock uplift rates across the orogen. Most of the accretionary flux is accommodated through the wet, windward side of the wedge, leading to a strong focusing of rock uplift rates there. This partitioning also means the sensitivity of the two-sided orogen is dominated by the sensitivity of the wet, windward flank. The only exception is where a high fraction of sediment eroded off the pro-wedge is recycled back into it, in which case the retro-wedge controls the sensitivity of the orogen, independent of the wind direction. See Whipple and Meade (2004) for a more extended discussion.

Lastly, the strength of the feedback is related to the response time of orogen. The ratio of the response times with and without the feedback is equal to the gain of the system.

10. DISCUSSION

All of the results follow as a necessary consequence of a self-similar form during orogen evolution. The degree to which natural orogens obey this is hard to know. Small orogenic belts at various convergent margins do approximate the critical-wedge form, and it is reasonable to suppose they have done so during the greater part of their history. However, at some level of detail, self-similarity cannot be rigorously adhered to as an orogen evolves: each new fold and thrust belt incorporated into an orogen, for example, adds new zones of weakness through which tectonic convergence may be more readily accommodated. Over the lifetime of the orogen the changing nature of the material within the orogen must affect both the internal strength and the erodibility of rocks at the surface: in thin-skinned fold and thrust belts, basal decolle-

ment is usually stratigraphically controlled and thus can be expected to be rotated to steeper angles over time due to isostatic compensation of crustal thickening (Boyer and Elliot, 1982).

Strict conformity to self-similarity is not necessary, however, for the feedbacks discussed here to still apply to an orogen. Fundamentally, the physical basis of the tectonic governor is that the characteristic orogen form (but importantly not the orogen size), remains approximately the same during orogen evolution. In other words, if an orogen builds up it also builds out. A variety of information can be used to evaluate the degree to which this is likely. Roe and Brandon (Critical form and feedbacks in mountain belt dynamics: the role of rheology as a tectonic governor, unpublished manuscript) explore the topographic form of an orogenic wedge for rheologies varying from Coulomb plastic to linear viscous: for Coulomb plastic rheology, as used here, $H \propto L$; for linear viscous rheology $H \propto L^{1/3}$. For this wide range of rheologies, Roe and Brandon show that the strength of the feedbacks varies by no more than a factor of two, and that the physical basis remains the same − the tectonic governor. Hoth (ms, 2006) shows for sandbox experiments under a variety of conditions appropriate to bivergent wedge settings that $H \propto L^{0.5 \text{ to } 0.7}$. The results of Roe and Brandon (Critical form and feedbacks in mountain belt dynamics: the role of rheology as a tectonic governor, unpublished manuscript) can be applied directly to argue that the strength of the feedbacks (as defined in this study) will be similar in such systems. In Taiwan, the gradual southward propagation of the convergence zone has produced a progressive southward evolution of the orogen growth (for example, Suppe, 1980; Stolar and others, 2007a), and the topographic form of the wedge is quite similar throughout the island (Stolar and others, 2007a). In this setting then, the action of a tectonic governor is strongly inferred. Another example, for the Nepalese Himalaya, Huntington and others (2006) use thermochronometer measurements to argue for an approximately five-fold increase in exhumation rates coincident with the onset of the late Pleistocene ice ages, while also inferring the basic topographic form of the Himalayas remains largely unchanged. Thus under a variety of numerical, laboratory, and actual settings, the operation of a tectonic governor is indicated.

The most robust and observable signature of climatic and tectonic controls on orogen dynamics is likely to be the partitioning of exhumation on the pro-and retro-flanks of the orogen. The results of the numerical modeling of Willett (1999a) conform to the predictions of (27) and figure 7 −they must do since the physics imposed in the integrations of the numerical model is very similar to that in analytical results presented here. Willett (1999a) also synthesizes some of the evidence for the sensitivity of exhumation patterns to the prevailing wind direction, contrasting the Olympics, Washington, (Brandon and others, 1998) with the Southern Alps in New Zealand (Tippet and Kamp, 1993). The observed exhumation rates in those orogens do show strong differences between the wet and dry flanks approximately in proportion to that predicted from (27). However even in these relatively straightforward settings, the interpretation of observed exhumation rates in terms of rock-uplift rates is complicated by lithological variations, horizontal advection of material within the orogen (for example, Stolar and others, 2005); and oblique convergence and glaciation (for example, Koons and others, 2003). More careful comparisons with numerical and physical models (for example, Hoth, ms, 2006; Naylor and Sinclair, 2007), and in more controlled settings would clearly be useful.

The feedbacks presented in this study were analyzed in the context of a steady-state mass balance between the accretionary and erosional fluxes. Even without this steady-state balance, provided that the time scale of interest is longer than that over which the deformation responds to changes in stresses, and longer than that over which the erosion adjusts to deformation of the landscape, the orogen will tend to

approximate a self-similar form and the feedbacks will apply. On million-year time scales these appear to be reasonable assumptions—they were the basis of the time-dependent studies of Whipple and Meade (2006) and Tomkin and Roe (2007), and are in agreement with the numerical results of Stolar and others (2006, 2007a).

We have also neglected glacial erosion. Calculations using a similar framework to this one show that the extreme case of a fully-glaciated orogen is more sensitive to precipitation than the fluvial case here (Tomkin and Roe, 2007). The reason is that glacial erosion laws depend more sensitively on the discharge of ice along a flow line than fluvial erosion depends on the discharge of water along a channel (for example, Hallet, 1979; Tomkin and Braun, 2002). In all other respects the feedbacks operate in the same way. In the perhaps more realistic case of an orogen experiencing episodic glaciations, the recurrence interval and the relative effectiveness of glacial and fluvial erosion become important (Hallet and others, 1996; Brocklehurst and Whipple, 2002; Montgomery and Greenberg, 2003). The insolation variations driven by 20 kyr precessional and 40 kyr obliquity orbital variations may be too rapid for landscapes at these scales to adjust (for example, Whipple, 2001; Tomkin, 2003), in which case it would be the average position of the equilibrium line altitude that would be the effective transition between the glacial and fluvial regimes. The inevitable onset of glaciation at sufficiently high elevations (for example, Broecker and Denton, 1990) is another climate feedback that we have not considered here.

The feedbacks demonstrated in this paper operate over a very large range of model parameter space, and their essential nature can be anticipated to apply for a wide range of different settings. Numerical models might be used to explore how incorporating more realistic physics such as temperature-dependent viscous deformation (for example, Willett and others, 1993), or strain-weakening at fault zones (for example, Beaumont and others, 1996), causes departure from self-similar evolution, and its consequent effect on the strength of the climatic and tectonic feedbacks (Roe and Brandon, Critical form and feedbacks in mountain belt dynamics: the role of rheology as a tectonic governor, unpublished manuscript). The approach presented here can be applied to other model parameters such as the rock erodibility and erosion exponents: similar perturbation analyses can be used to relax the assumptions that model parameters are constant and independent of tectonic and climatic forcing, or orogen scale. As more information emerges from techniques such as thermochronometry and tectonic geomorphology, patterns of exhumation and their changes over time will increasingly be revealed. It is to be hoped that comparisons of such observations with idealized analyses like the one presented here will afford greater insight into the processes at work in orogen dynamics. Such comparisons are only just beginning. What is already clear is that, by combining carefully targeted observations with theoretical and numerical modeling, there is still a lot of progress to be made in understanding the rich interactions occurring in what is one of the archetypal Earth Systems.

APPENDIX A

Feedback Analysis for Two-Sided Critical Wedge

In this Appendix we derive expressions for the system sensitivity, gains and feedback factors for the two-sided critical wedge framework, shown schematically in figure 6.

(24) and (25) can be combined into a general scaling relationship of the form $F = F(L_p, L_r, P_p, P_r)$. A first order Taylor series expansion can then be written

$$\Delta F = \frac{\partial F}{\partial L_p} \Delta L_p + \frac{\partial F}{\partial L_r} \Delta L_r + \frac{\partial F}{\partial P_p} \Delta P_p + \frac{\partial F}{\partial P_r} \Delta P_r. \tag{A-1}$$

First, assuming that P_p and P_r are constant, then substitution of (25) and the derivative of (24) into A-1 gives

$$\Delta F = (1 - \xi)(1 + hm)\frac{F_p}{L_p}\Delta L_p + (1 + hm)\frac{F_p}{L_r}\Delta L_r. \tag{A-2}$$

From (26), $\Delta L_p / L_p = \Delta L_r / L_r = \Delta L / L$. Upon subsitution of this and (25) into (A-2) and simplifying, the width sensitivity factor for the two-sided wedge with no precipitation feedback reduces to

$$\lambda_L^0 = \frac{\Delta L}{\Delta F} = \frac{L}{F}\frac{1}{(1 + hm)}. \tag{A-3}$$

The width sensitivity for the two-sided wedge is therefore the same as for the one-sided wedge, as might be expected from the self-similar evolution of the two flanks. It is also a formal demonstration of why the scaling relationships found by Whipple and Meade (2004) and Roe and others (2006) are the same.

Allowing now for a precipitation feedback, the extra terms in (A-1) can be expressed as $\partial F / \partial P_p = (1 - \xi) m F_p / P_p$ and $\partial F / \partial P_r = m F_r / P_r$. Then, using $\Delta P_p = (\partial P_p / \partial L)\Delta L$ and a similar expression for ΔP_r, (A-1) becomes

$$\Delta F = (1 + hm)\frac{F}{L}\Delta L + \left\{(1 - \xi)m\frac{F_p}{L_p}\frac{\partial P_p}{\partial L} + m\frac{F_r}{P_r}\frac{\partial P_r}{\partial L}\right\}\Delta L. \tag{A-4}$$

So, finally, the width sensitivity factor with a precipitation feedback can be written in terms of the width sensitivity factor without a feedback:

$$\lambda_L = \frac{\lambda_L^0}{1 + m\lambda_L^0\left[(1 - \xi)\frac{F_p}{P_p}\frac{\partial P_p}{\partial L} + \frac{\boldsymbol{F_r}}{P_r}\frac{\partial P_r}{\partial L}\right]}. \tag{A-5}$$

References

Adams, J., 1980, Contemporary uplift and erosion of the Southern Alps, New Zealand: Bulletin of the Geological Society of America, Part I, v. 91, p. 1–114.
Anders, A. M., Roe, G. H., Durran, D. R., and Minder, J. U., 2007, Small scale special Gradients in Climatological precipitation in the Olympic Peninsula: Journal of Hydrometeorology, v. 8, p. 1068–1081.
Beaumont, C., Fullsack, P., and Hamilton, J., 1992, Erosional control of active compressional orogens, *in* McClay, K. R., editor, Thrust Tectonics: New York, Chapman Hall, p. 1–18.
Beaumont, C., Kamp, P. J. J., Hamilton, J., and Fullsack, P., 1996, The continental collision cones, South Island, New Zealand: Comparison of geodynamical models and observations: Journal of Geophysical Research, v. 101, No. B2, p. 3333–3359, doi:10.1029/95JB02401.
Blumen, W., editor, 1990, Atmospheric Processes Over Complex Terrain: Boston, Massachusetts, American Meterological Society, Meteorological Monographs, v. 23, No. 45, 323 p.
Bode, H. W., 1945, Network analysis and feedback amplifier design: New York, Van Nostrand, 577 p.
Boyer, S. E., and Elliot, D., 1982, Thrust systems: American Association of Petroleum Geologists Bulletin, v. 66, p. 1196–1230.
Brandon, M. T., Roden-Tice, M. K., and Garver, J. I., 1998, Late Cenozoic exhumation of the Cascadia accretionary wedge in the Olympic Mountains, northwest Washington State: Bulletin of the Geological Society of America, v. 110, p. 985–1009, doi:10.1130/0016-7606(1998)110<0985:LCEOTC2.3.CO;2.
Brocklehurst, S. H., and Whipple, K. X., 2002, Glacial erosion and relief production in the Eastern Sierra Nevada, California: Geomorphology, v. 42, p. 1–24, doi:10.1016/S0169-555X(01)00069-1.
Broecker, W. S., and Denton, G. H., 1990, The role of ocean-atmosphere reorganizations in glacial cycles: Quaternary Science Reviews, v. 9, p. 305–341, doi:10.1016/0277-3791(90)90026-7.
Brophy, J. J., 1983, Basic electronics for scientists: New York, McGraw-Hill, 454 p.
Brozovic, N., Burbank, D. W., and Meigs, A. J., 1997, Climatic limits on landscape development in the northwestern Himalaya: Science, v. 276, p. 571–574, doi:10.1126/science.276.5312.571.
Chapple, W. M., 1978, Mechanics of thin-skinned fold-and-thrust belts: Geological Society of America Bulletin, v. 89, p. 1189–98, doi:10.1130/0016-7606(1978)891189:MOTFB2.0.CO;2.

Costa, J. E., and O'Conner, J. E., 1995, Geomorphically effective floods, *in* Costa, J. E., Miller, A. J., Potter, K. W., and Wilcock, P. R., editors, Natural and Anthropogenic influences in fluvial geomorphology: The Wolman Volume: Washington, D. C., American Geophysical Union, Geophysical Monograph Series, v. 89, p. 45–56.

Dahlen, F. A., 1984, Noncohesive Critical Coulomb Wedges: An Exact Solution: Journal of Geophysical Research, v. 89, B12, p. 10125–10133, doi:10.1029/JB089iB12p10125.

——— 1990, Critical taper model of fold-and-thrust belts and accretionary wedges: Annual Review of Earth and Planetary Sciences, v. 18, p. 55–99, doi:10.1146/annurev.ea.18.050190.000415.

Davis, D., Suppe, J., and Dahlen, F. A., 1983, Mechanics of fold-and-thrusts belts and accretionary wedges: Journal of Geophysical Research, v. 88, No. B2, p. 1153–1172, doi:10.1029/JB088iB02p01153.

Delaney, C. F. G., 1969, Electronics for the physicist: Baltimore, Maryland, Penguin, 256 p.

Hack, J. T., 1957, Studies of longitudinal stream profiles in Virginia and Maryland: U.S. Geological Survey Professional Paper 294-B, 94, 97 p.

Hallet, B., 1979, A theoretical model of glacial abrasion: Journal of Glaciology, v. 23, p. 39–50.

Hallet, B., Hunter, L., and Bogen, J., 1996, Rates of erosion and sediment evacuation by glaciers: A review of field data and their implications: Global and Planetary Change, v. 12, p. 213–235, doi:10.1016/0921-8181(95)00021-6.

Hansen, J., Lacis, A., Rind, D., Russell, G., Stone, P., Fung, I., Ruedy, R., and Lerner, J., 1984, Climate sensitivity: Analysis of feedback mechanisms, *in* Hansen, J. E., and Takahashi, T., editors, Climate Processes and Climate Sensitivity: American Geophysical Union, Geophysical Monograph 29, p. 130–163.

Hilley, G. E., Strecker, M., and Ramos, V. A., 2004, Growth and erosion of fold-and-thrust belts with an application to the Aconcagua Fold–and–Thrust Belt, Argentina: Journal of Geophysical Research, v. 109, B01410, doi: 10.1029/2002JB002282, doi:10.1029/2002JB002282.

Hoth, S., ms, 2006, Deformation, erosion and natural resources in continental collision zones: Insight from scaled sandbox simulations: Berlin, Germany, Fachbereich Geowissenschaften, Freie Universität Berlin, Ph. D. thesis, 142 p.

Kageyama, M., Valdes, P. J., Ramstein, G., Hewitt, C., and Wyputta, U., 1999, Northern Hemisphere Storm Tracks in Present Day and Last Glacial Maximum Climate Simulations: A Comparison of the European PMIP models: Journal of Climate, v. 12, p. 742–760, doi:10.1175/1520-0442(1999)012<0742:NHSTIP>2.0.CO;2.

Koons, P. O., 1989, The topographic evolution of collisional mountain belts: A numerical look at the Southern Alps, New Zealand: American Journal of Science, v. 289, p. 1041–1069.

——— 1990, The two-sided orogen: Collision and erosion from the sandbox to the Southern Alps: Geology, v. 18, p. 679–682, doi:10.1130/0091-7613(1990)018<0679:TSOCAE>2.3.CO;2.

Koons, P. O, Norris, R. J., Craw, D., and Cooper, A. F., 2003, Influence of exhumation on the structural evolution of transpressional plate boundaries: An example from the Southern Alps, New Zealand: Geology, v. 31, p. 3–6, doi:10.1130/0091-7613(2003)031<0003:IOEOTS>2.0.CO;2.

Masek, J. G., Isacks, B. L., Gubbels, T. L., and Fielding, E. J., 1994, Erosion and tectonics at the margins of continental plateaus: Journal of Geophysical Research, v. 99, No. B7, p. 13,941–13,956, doi:10.1029/94JB00461.

Maxwell, J. C., 1868, On Governors: Proceedings of the Royal Society, v. 16, p. 270–283, doi:10.1098/rspl.1867.0055.

Montgomery, D. R., and Dietrich, W. E., 1992, Channel initiation and the problem of landscape scale: Science, v. 255, No. 5046, p. 826–830, doi: 10.1126/science.255.5046.826.

Montgomery, D. R., Balco, G., and Willett, S. D., 2001, Climate, tectonics, and the morphology of the Andes: Geology, v. 29, p. 579–582, doi:10.1130/0091-7613(2001)029<0579:CTATMO>2.0.CO;2.

Naylor, M., and Sinclair, H. D., 2007, Punctuated thrust deformation in the context of doubly vergent thrust wedges: Implications for the localization of uplift and exhumation: Geology, v. 35, p. 559–562, doi:10.1130/G23448A.1.

Reiners, P. W., and Brandon, M. T., 2006, Using thermochronology to understand orogenic erosion: Annual Review of Earth and Planetary Sciences, v. 34, p. 419–466.

Reiners, P. W., Ehlers, T. A., Mitchell, S. G., and Montgomery, D. R., 2003, Coupled spatial variations in precipitation and long-term erosion rates across the Washington Cascades: Nature, v. 426, p. 645–647, doi:10.1038/nature02111.

Riesner, J., Rasmussen, R. M., and Bruintjes, R. T., 1998, Explicit forecasting of supercooled liquid water in winter storms using the MM5 mesoscale model: Quarterly Journal of the Royal Meteorological Society, v. 124, p. 1071–1107, doi:10.1002/qj.49712454804.

Roe, G. H., 2005, Orographic precipitation: Annual Review of Earth and Planetary Sciences, v. 33, p. 645–671, doi:10.1146/annurev.earth.33.092203.122541.

Roe, G. H., and Baker, M. B., 2006, Microphysical and geometrical controls on the pattern of orographic precipitation: Journal of the Atmospheric Sciences, v. 63, p. 861–880, doi:10.1175/JAS3619.1.

——— M. B., 2007, Why is climate sensitivity so unpredictable?: Science, v. 318, p. 629–632, doi:10.1126/science.1144735.

Roe, G. H., Stolar, D. B., and Willett, S. D., 2006, Response of a steady-state critical wedge orogen to changes in climate and tectonic forcing, *in* Willett, S. D., Hovius, N., Brandon, M., and Fisher, D. M., editors, Tectonics, Climate, and Landscape Evolution: Boulder, Colorado, Geological Society of America Special Paper 398, p. 227–249, doi:10/1130/2005.2398(13).

Ruhl, K. W., and Hodges, K. V., 2005, The use of detrital mineral cooling ages to evaluate steady-state assumptions in active orogens: An example from the central Nepalese Himalaya: Tectonics, v. 24, TC4015.

Schlesinger, M. E., 1985, Feedback analysis of results from energy balance and radiative-convective models, *in* MacCracken, M. C., and Luther, F. M., editors, The Potential Climatic Effects of Increasing Carbon Dioxide: U.S. Department of Energy, DOE/ER-0237, p. 280–319.

Smith, R. B., 1979, The influence of mountains on the atmosphere: Advances in Geophysics, v. 21, p. 87–230.

—— 2006, Progress on the theory of orographic precipitation, *in* Willett, S. D., Hovius, N., Brandon, M. T., and Fisher, D. M., editors, Tectonics, Climate, and Landscape Evolution: Boulder, Colorado, Penrose Conference Series, Geological Society of America Special Paper 398, p. 1–16, doi: 10.1130/2006.2398(01).

Smith, R. B., and Barstad, I., 2004, A linear theory of orographic precipitation: Journal of the Atmospheric Sciences, v. 61, p. 1377–1391, doi:10.1175/1520-0469(2004)061<1377:ALTOOP>2.0.CO;2.

Stolar, D. B., Roe, G. H., and Willett, S. D., 2005, Reconciling observations and theory of erosion rate patterns in the Olympic Mountains of Washington State: EOS, Transactions of the American Geophysical Union Fall meeting, San Francisco, California.

Stolar, D. B., Willett, S. D., and Roe, G. H., 2006, Climatic and tectonic forcing of a critical orogen: Findings from a numerical sandbox, *in* Willett, S. D., Hovius, N., Brandon, M. T., and Fisher, D. M., editors, Tectonics, Climate, and Landscape Evolution: Boulder, Colorado, Penrose Conference Series, Geological Society of America Special Paper 398, p. 241–250, doi:10.1130/2006.2398(14).

Stolar, D. R., Roe, G. H., and Willett, S. D., 2007a, Controls on the patterns of topography and erosion rate in a critical orogen: Journal of Geophysical Research, v. 112, F04002, doi:10.1029/2006JF000713.

Stolar, D. B., Willett, S. D., and Montgomery, D. R., 2007b, Characterization of topographic steady state in Taiwan: Earth and Planetary Science Letters, v. 261, p. 421–431, doi:10.1016/j.epsl.2007.07.045.

Suppe, J., 1980, A retrodeformable cross section of northern Taiwan: Geological Society of China Proceedings, v. 23, p. 46–55.

Tippett, J. M., and Kamp, P. J. J., 1993, Fission Track Analysis of the Late Cenozoic Vertical Kinematics of Continental Pacific Crust, South Island, New Zealand: Journal of Geophysical Research, v. 98, No. B9, p. 16,119–16,148, doi:10.1029/92JB02115.

Tomkin, J. H., 2003, Erosional feedbacks and the oscillation of ice masses: Journal of Geophysical Research, v. 108, No. B10, p. 2488, doi:10.1029/2002JB002087.

Tomkin, J. H., and Braun, J., 2002, The influence of alpine glaciation on the relief of tectonically active mountain belts: American Journal of Science, v. 302, p. 169–190, doi:10.2475/ajs.302.3.169.

Tomkin, J. H., and Roe, G. H., 2007, Climate and tectonic controls on glaciated critical-taper orogens: Earth and Planetary Science Letters, v. 262, p. 385–397.

Torn, M. S., and Harte, J., 2006: Missing feedbacks, asymmetric uncertainties, and the underestimation of future warming: Geophysical Research Letters, v. 33, L10703, doi:10.1029/2005GL025540.

Tucker, G. E., and Bras, R. L., 2000, A stochastic approach to modeling the role of rainfall variability in drainage basin evolution: Water Resources Research, v. 36, p. 1953–1964, doi:10.1029/2000WR900065.

Whipple, K. X., 2001, Fluvial landscape response time: How plausible is steady state denudation?: American Journal of Science, v. 301, p. 313–325.

—— 2004, Bedrock rivers and the geomorphology of active orogens: Annual Review of Earth and Planetary Sciences, v. 32, p. 151–185, doi:10.1146/annurev.earth.32.101802.120356.

Whipple, K. X., and Meade, B. J., 2004, Controls on the strength of coupling among climate, erosion, and deformation in two-sided, frictional orogenic wedges at steady state: Journal of Geophysical Research, v. 109, F01011, doi:10.1029/2003JF000019.

—— 2006, Orogen Response to Changes in Climatic and Tectonic Forcing: Earth and Planetary Science Letters, v. 243, p. 218–228, doi:10.1016/j.epsl.2005.12.022.

Whipple, K. X., and Tucker, G. E., 1999, Dynamics of the stream-power river incision model: Implications for height limits of mountain ranges, landscape response time scales, and research needs: Journal of Geophysical Research, v. 104, No. B8, p. 17,661–17,674, doi:10.1029/1999JB900120.

Whipple, K. X., Kirby, E., and Brocklehurst, S. H., 1999, Geomorphic limits to climate-induced increases in topographic relief: Nature, v. 401, p. 39–43, doi:10.1038/43375.

Willett, S. D., 1999a, Orogeny and orography: The effects of erosion on the structure of mountain belts: Journal of Geophysical Research, v. 104, No. B12, p. 28,957–28,981, doi:10.1029/1999JB900248.

—— 1999b, Rheological dependence of extension in wedge models of convergent orogens: Tectonophysics, v. 305, p. 419–435, doi:10.1016/S0040-1951(99)00034-7.

Willett, S. D., Beaumont, C., and Fullsack, P., 1993, Mechanical model for the tectonics of doubly-vergent compressional orogens: Geology, v. 21, p. 371–374, doi:10.1130/0091-7613(1993)021<0371:MMFTTO>2.3.CO;2.

Wratt, D. S., Revell, M. J., Sinclair, M. R., Gray, W. R., Henderson, R. D., and Chater, A. M., 2000, Relationships between air mass properties and mesoscale rainfall in New Zealand's Southern Alps: Atmospheric Research, v. 52, p. 261–282, doi:10.1016/S0169-8095(99)00038-1.